US009270384B2

(12) **United States Patent**
Bisplinghoff et al.

(10) **Patent No.: US 9,270,384 B2**
(45) **Date of Patent: Feb. 23, 2016**

(54) **SUB-SAMPLED CARRIER PHASE RECOVERY**

(71) Applicant: **Cisco Technology, Inc.**, San Jose, CA (US)

(72) Inventors: **Andreas Bisplinghoff**, Hallerndorf (DE); **Chris Fludger**, Nuremberg (DE)

(73) Assignee: **Cisco Technology, Inc.**, San Jose, CA (US)

(*) Notice: Subject to any disclaimer, the term of this patent is extended or adjusted under 35 U.S.C. 154(b) by 79 days.

(21) Appl. No.: **14/154,674**

(22) Filed: **Jan. 14, 2014**

(65) **Prior Publication Data**

US 2015/0200731 A1 Jul. 16, 2015

(51) **Int. Cl.**

H04B 10/06	(2006.01)
H04B 10/61	(2013.01)
H04L 7/00	(2006.01)
H04L 7/04	(2006.01)

(52) **U.S. Cl.**

CPC ***H04B 10/6165*** (2013.01); ***H04L 7/0075*** (2013.01); ***H04L 7/048*** (2013.01)

(58) **Field of Classification Search**

CPC H04B 10/6165; H04B 10/079; H04L 7/0075; H04L 7/048
USPC 398/208
See application file for complete search history.

(56) **References Cited**

U.S. PATENT DOCUMENTS

8,693,897	B2 *	4/2014	Mo et al.	398/208
2014/0169784	A1 *	6/2014	Zhou	398/25

OTHER PUBLICATIONS

Gao et al "Low-Complexity Two-Stage Carrier Phase Estimation for 16-QAM Systems using QPSK Partitoning and Maximum Likelihood Detection", Optical Fiber Communication Conference, Mar. 2011, 3 pages.*

Rasmussen et al., "Digital Coherent Receiver Technology for 100-GB/s Optical Transport Systems", Fujitsu Sci. Tech, J. vol. 46, No. 1, pp. 63-71, Jan. 2010.*

Bisplinghoff, et al., "Carrier and Phase Recovery Algorithms for QAM Constellations: Real-time Implementations," Signal Processing in Photonic Communications (SPPCom), Jul. 2013, 3 pages.

Gao, et al., "Low-Complexity Two-Stage Carrier Phase Estimation for 16-QAM Systems using QPSK Partitioning and Maximum Likelihood Detection," Optical Fiber Communication Conference, Mar. 2011, 3 pages.

Rasmussen, et al., "Digital Coherent Receiver Technology for 100-Gb/s Optical Transport Systems," Fujitsu Sci. Tech. J., vol. 46, No. 1, pp. 63-71, Jan. 2010.

* cited by examiner

Primary Examiner — M. R. Sedighian

(74) *Attorney, Agent, or Firm* — Edell, Shapiro & Finnan, LLC

(57) **ABSTRACT**

Presented herein are sub-sampled carrier phase recovery techniques. In accordance with one example, a plurality of consecutive symbols associated with a received optical signal is obtained. Carrier phase recovery of the optical signal is performed using one or more carrier phase estimation stages. At each of the one or more carrier phase estimation stages, a subset of the plurality of consecutive symbols is selected for use in carrier phase estimation. The subset of symbols selected for use in carrier phase estimation at each of the one or more stages comprises symbols that provide the most phase recovery information for each of the one or more stages.

20 Claims, 8 Drawing Sheets

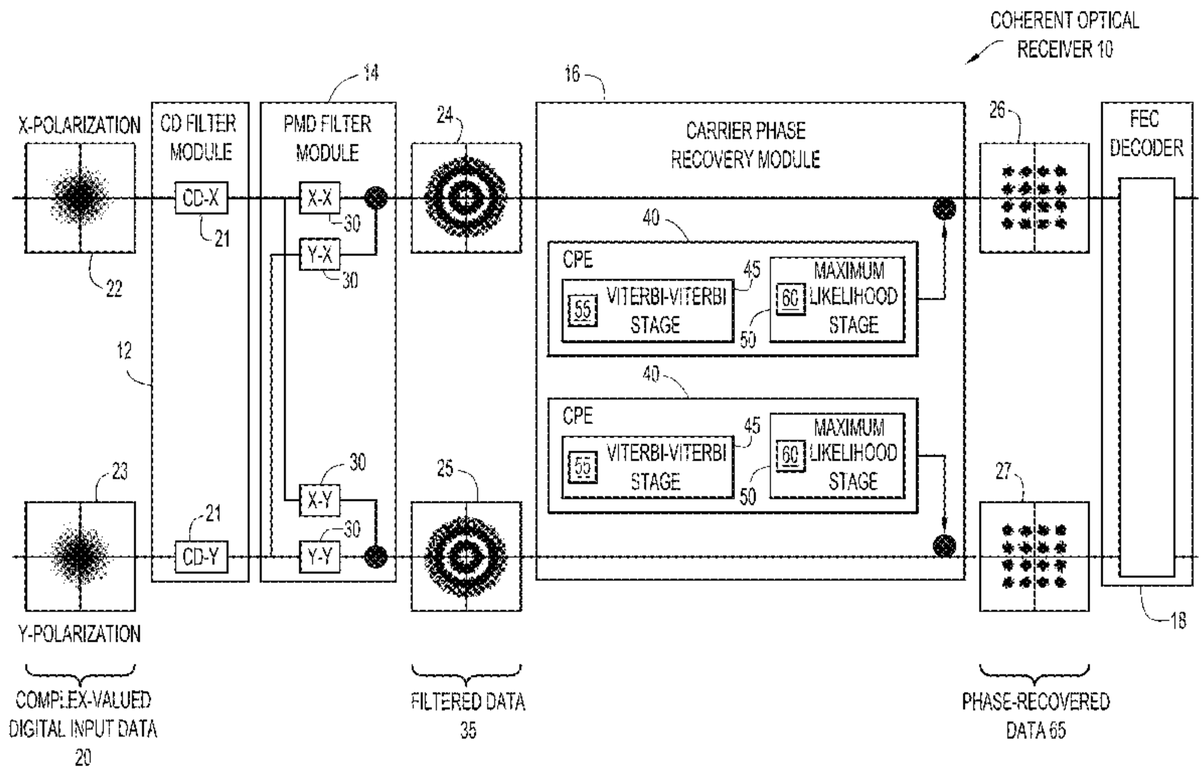

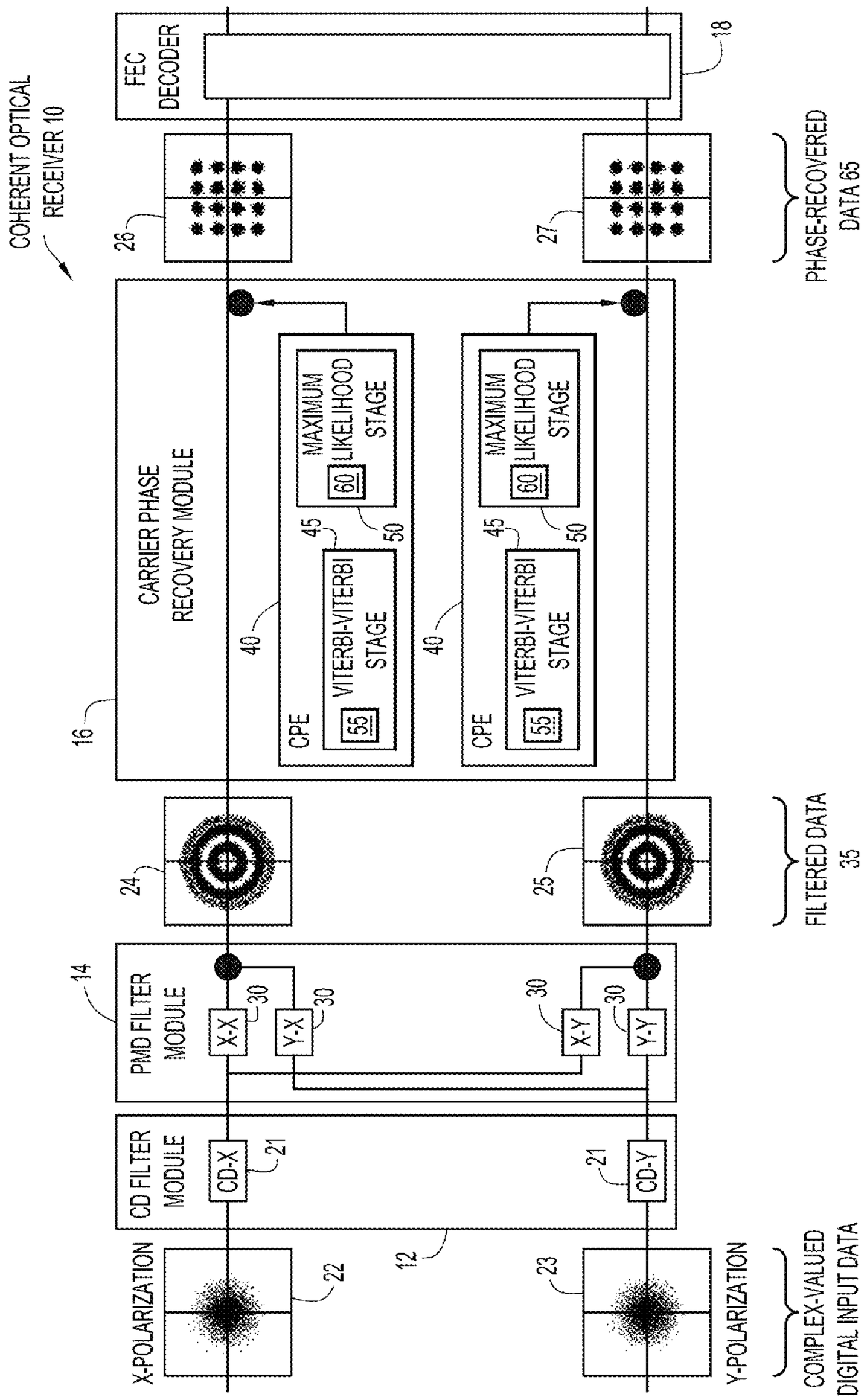
COHERENT OPTICAL RECEIVER 10
FEC DECODER
18
26
27
PHASE-RECOVERED DATA 65
CARRIER PHASE RECOVERY MODULE
16
MAXIMUM LIKELIHOOD STAGE
60
45
50
CPE
40
VITERBI-VITERBI STAGE
55
24
25
FILTERED DATA 35
PMD FILTER MODULE
14
X-X
Y-X
X-Y
Y-Y
30
CD FILTER MODULE
CD-X
CD-Y
21
12
22
23
X-POLARIZATION
Y-POLARIZATION
COMPLEX-VALUED DIGITAL INPUT DATA 20

FIG.1

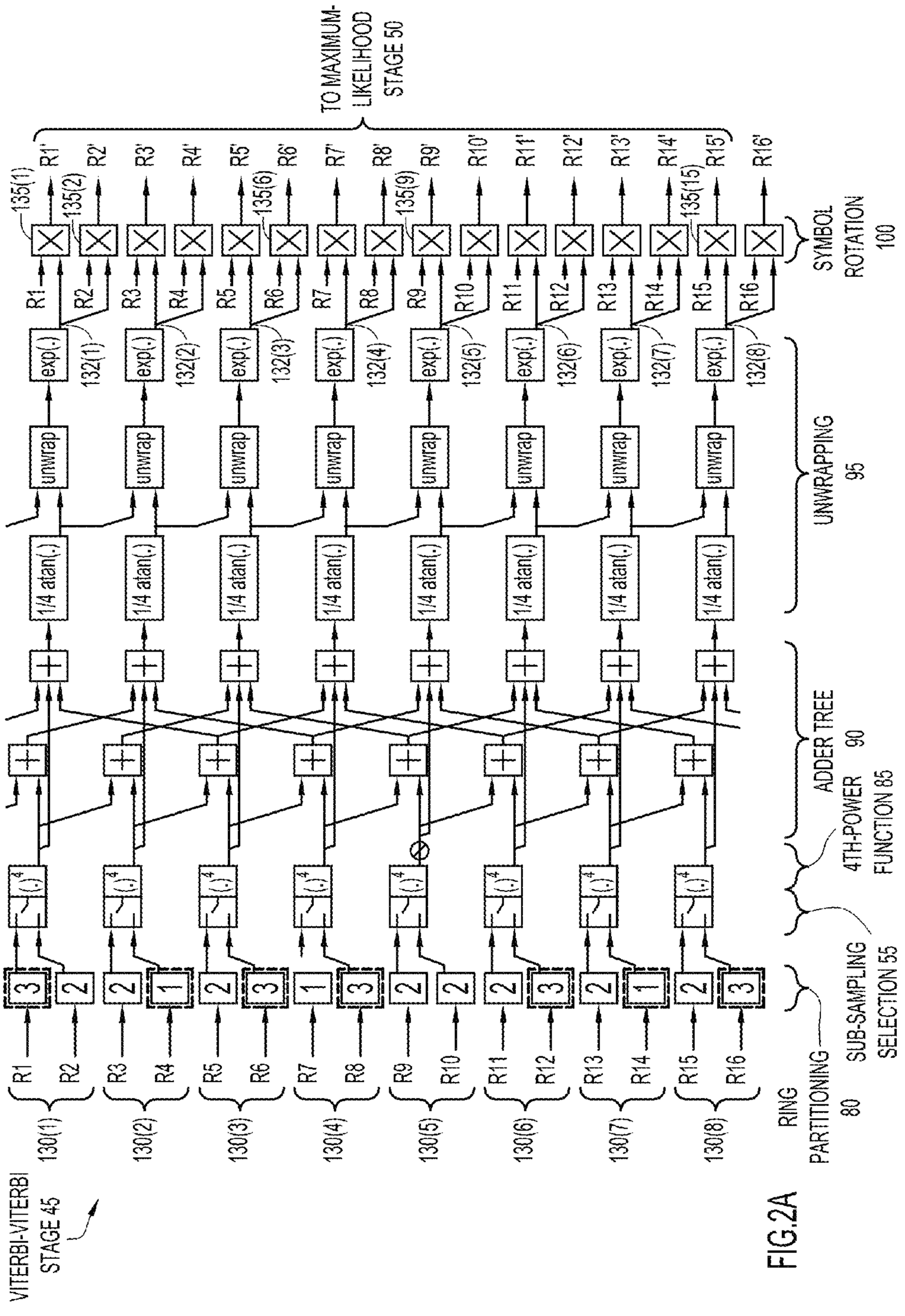
TO MAXIMUM-LIKELIHOOD STAGE 50
R1' R2' R3' R4' R5' R6' R7' R8' R9' R10' R11' R12' R13' R14' R15' R16'
135(1) 135(2) 135(6) 135(9) 135(15)
SYMBOL ROTATION 100
R1 R2 R3 R4 R5 R6 R7 R8 R9 R10 R11 R12 R13 R14 R15 R16
exp(.) 132(1) 132(2) 132(3) 132(4) 132(5) 132(6) 132(7) 132(8)
unwrap
1/4 atan(.)
UNWRAPPING 95
ADDER TREE
4TH-POWER 90
FUNCTION 85
R1 R2 R3 R4 R5 R6 R7 R8 R9 R10 R11 R12 R13 R14 R15 R16
130(1) 130(2) 130(3) 130(4) 130(5) 130(6) 130(7) 130(8)
VITERBI-VITERBI STAGE 45
RING PARTITIONING 80
SUB-SAMPLING SELECTION 55

FIG.2A

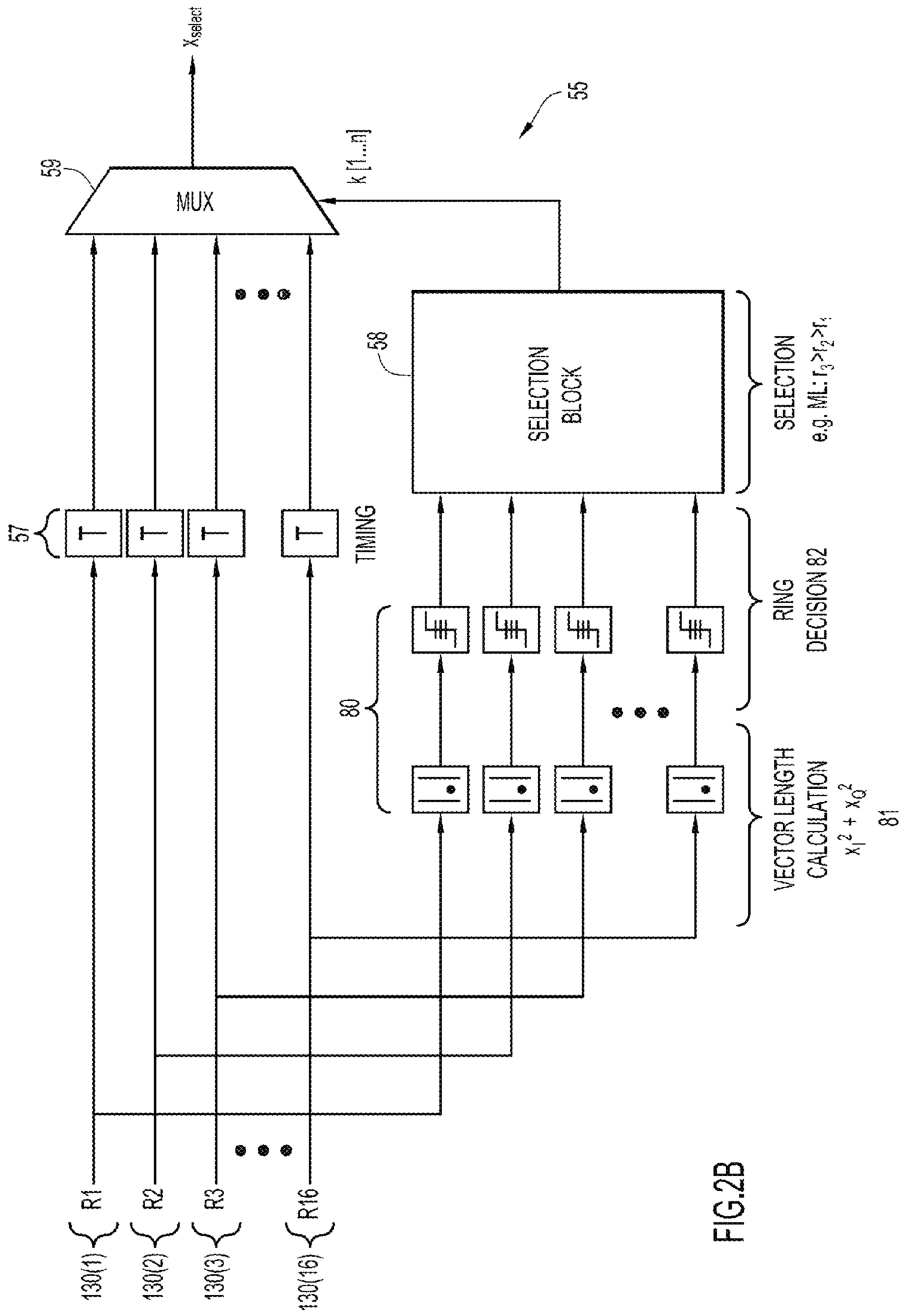
Xselect
55
59
MUX
k [1...n]
58
SELECTION BLOCK
SELECTION
e.g. ML: r3>r2>r1
57
T
TIMING
80
RING DECISION 82
VECTOR LENGTH CALCULATION
XI2 + XQ2
81
R1
R2
R3
R16
130(1)
130(2)
130(3)
130(16)

FIG.2B

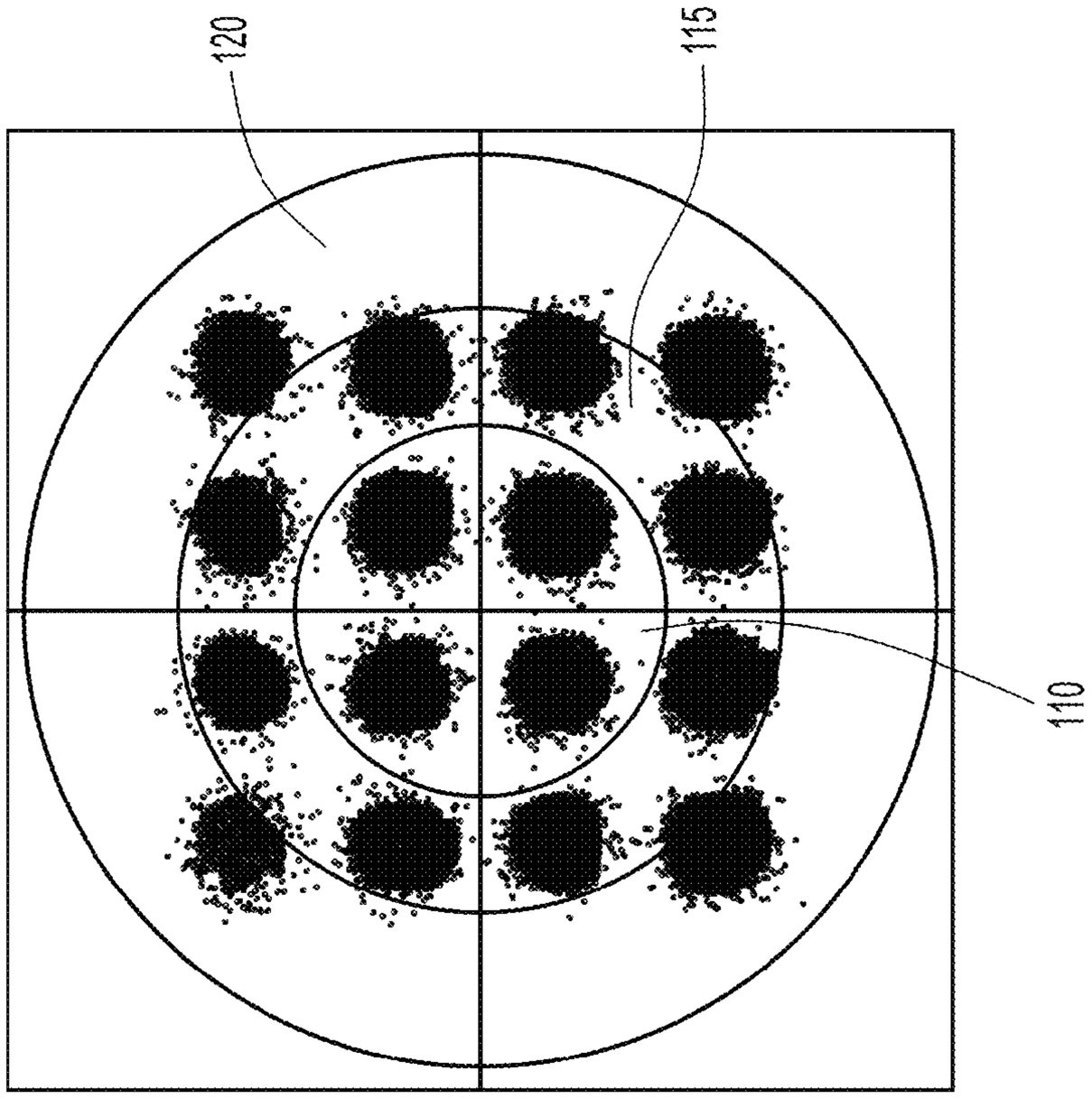

FIG.3

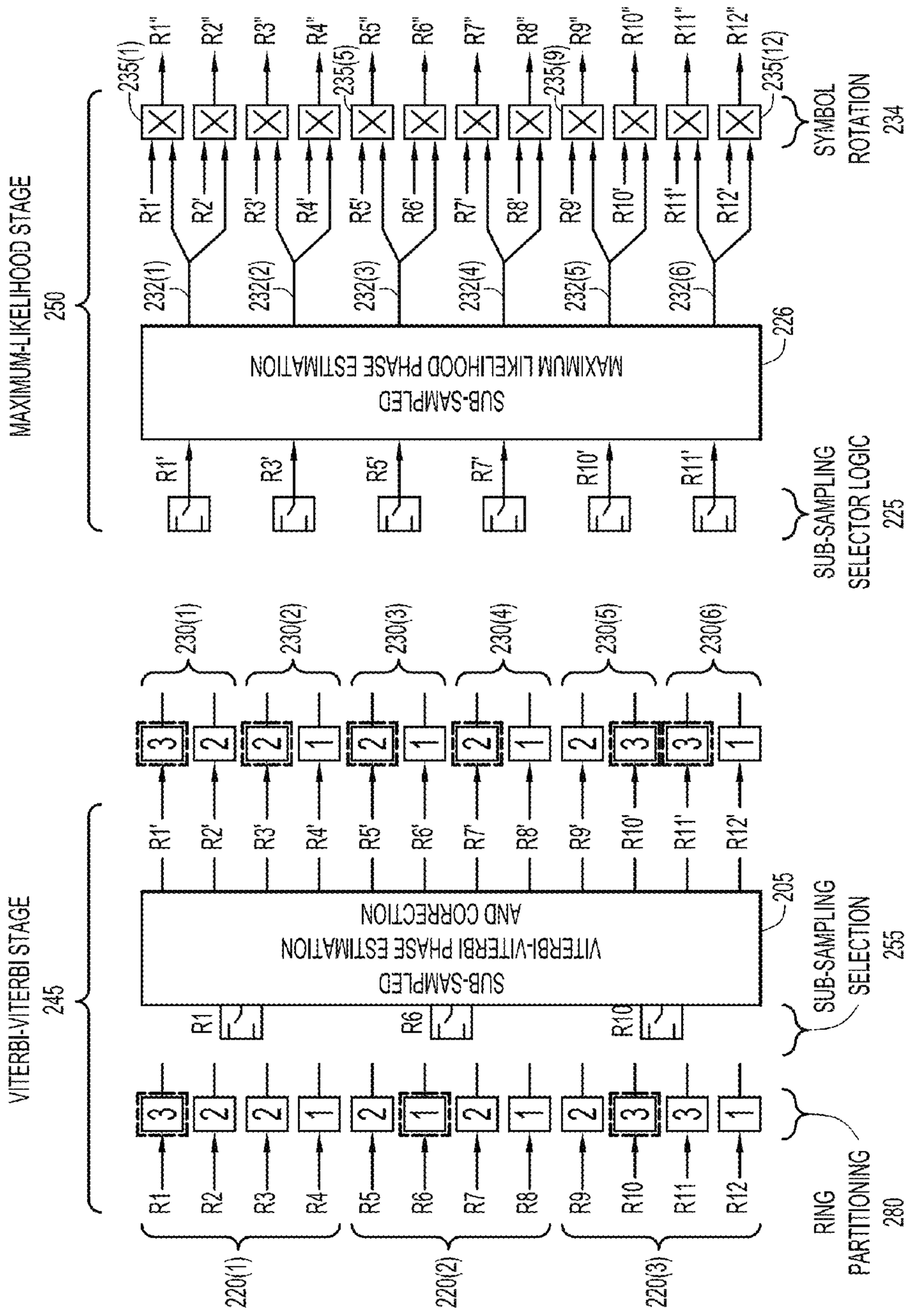
MAXIMUM-LIKELIHOOD STAGE
250
SUB-SAMPLED
MAXIMUM LIKELIHOOD PHASE ESTIMATION
226
SUB-SAMPLING
SELECTOR LOGIC
225
SYMBOL
ROTATION
234
VITERBI-VITERBI STAGE
245
SUB-SAMPLED
VITERBI-VITERBI PHASE ESTIMATION
AND CORRECTION
205
SUB-SAMPLING
SELECTION
255
RING
PARTITIONING
280

FIG.4

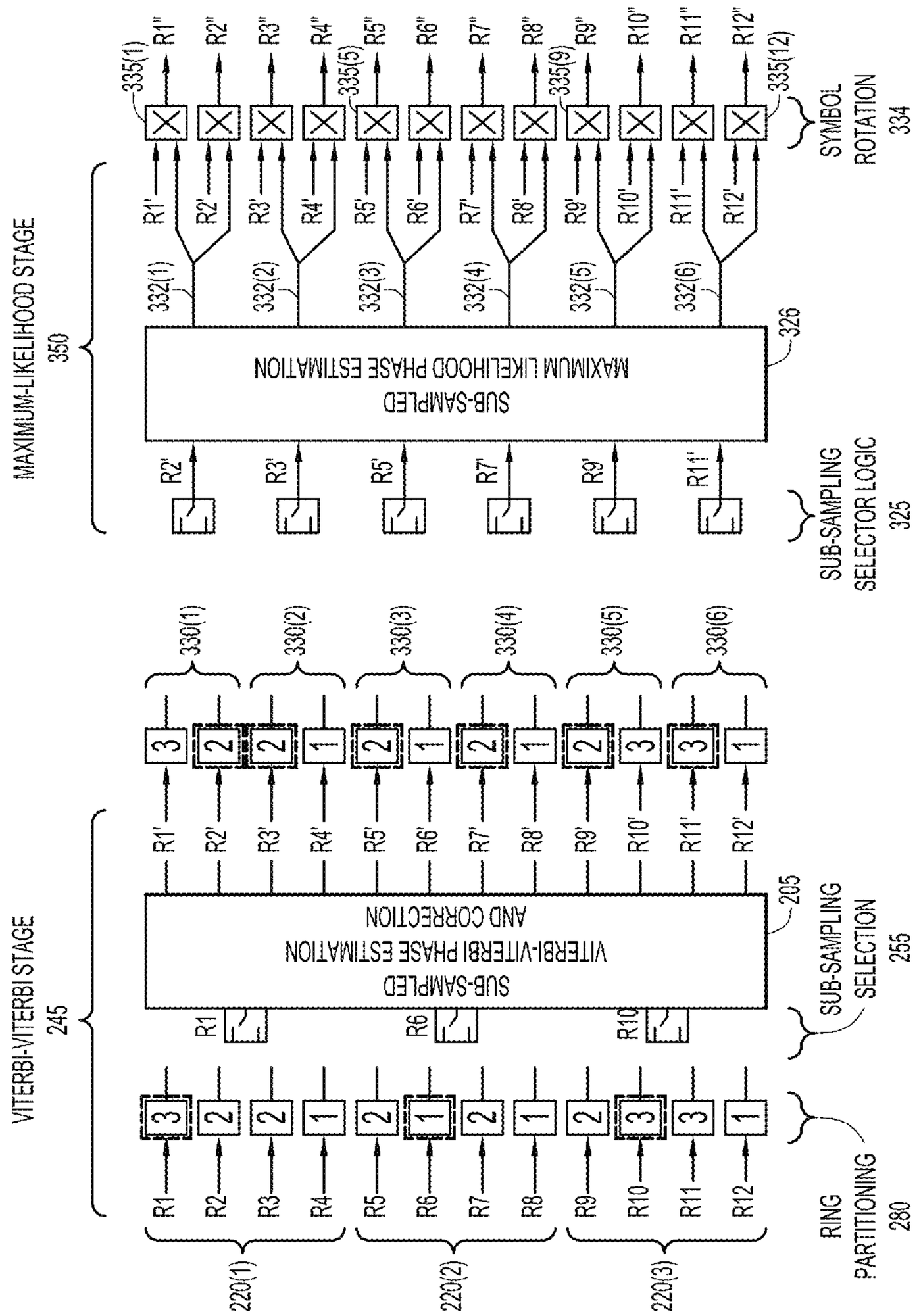
VITERBI-VITERBI STAGE
245
SUB-SAMPLED
VITERBI-VITERBI PHASE ESTIMATION
AND CORRECTION
205
SUB-SAMPLING
SELECTION
255
R1
R6
R10
R1' R2' R3' R4' R5' R6' R7' R8' R9' R10' R11' R12'
330(1) 330(2) 330(3) 330(4) 330(5) 330(6)
3 2 2 1 2 1 2 1 2 3 3 1
R1 R2 R3 R4 R5 R6 R7 R8 R9 R10 R11 R12
220(1) 220(2) 220(3)
RING
PARTITIONING
280
MAXIMUM-LIKELIHOOD STAGE
350
SUB-SAMPLED
MAXIMUM LIKELIHOOD PHASE ESTIMATION
326
R2' R3' R5' R7' R9' R11'
SUB-SAMPLING
SELECTOR LOGIC
325
R1' R2' R3' R4' R5' R6' R7' R8' R9' R10' R11' R12'
332(1) 332(2) 332(3) 332(4) 332(5) 332(6)
335(1) 335(5) 335(9) 335(12)
R1" R2" R3" R4" R5" R6" R7" R8" R9" R10" R11" R12"
SYMBOL
ROTATION
334

FIG.5

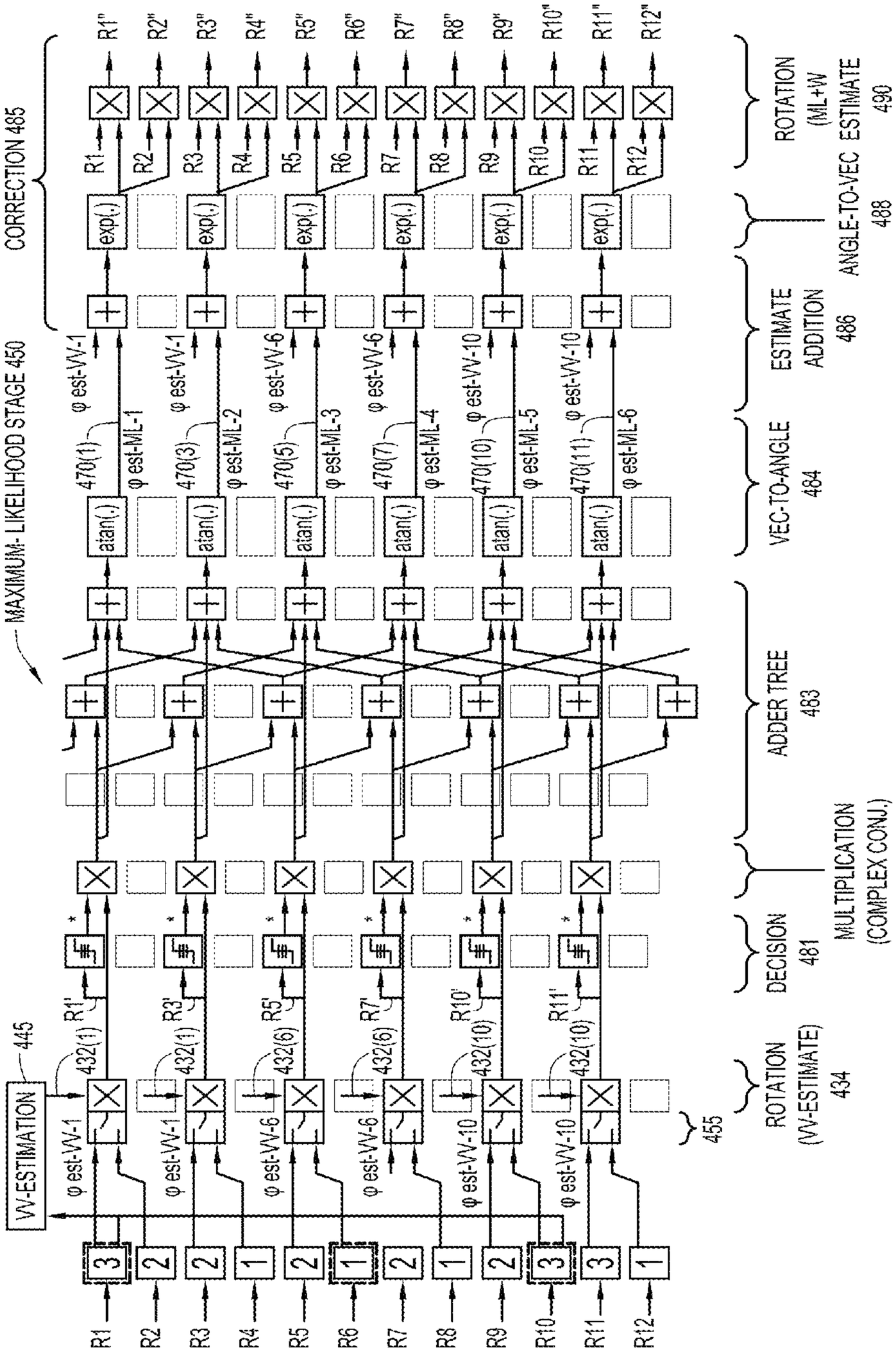
CORRECTION 485
MAXIMUM- LIKELIHOOD STAGE 450
VV-ESTIMATION 445
ROTATION (ML+W) ESTIMATE 490
ANGLE-TO-VEC ESTIMATE 488
VEC-TO-ANGLE 484
ESTIMATE ADDITION 486
ADDER TREE 483
MULTIPLICATION (COMPLEX CONJ.) 482
DECISION 481
ROTATION (VV-ESTIMATE) 434
455
exp(.)
atan(.)
φ est-ML-1
φ est-ML-2
φ est-ML-3
φ est-ML-4
φ est-ML-5
φ est-ML-6
φ est-VV-1
φ est-VV-6
φ est-VV-10
470(1)
470(3)
470(5)
470(7)
470(10)
470(11)
432(1)
432(6)
432(10)
R1
R2
R3
R4
R5
R6
R7
R8
R9
R10
R11
R12
R1'
R3'
R5'
R7'
R10'
R11'

FIG.6

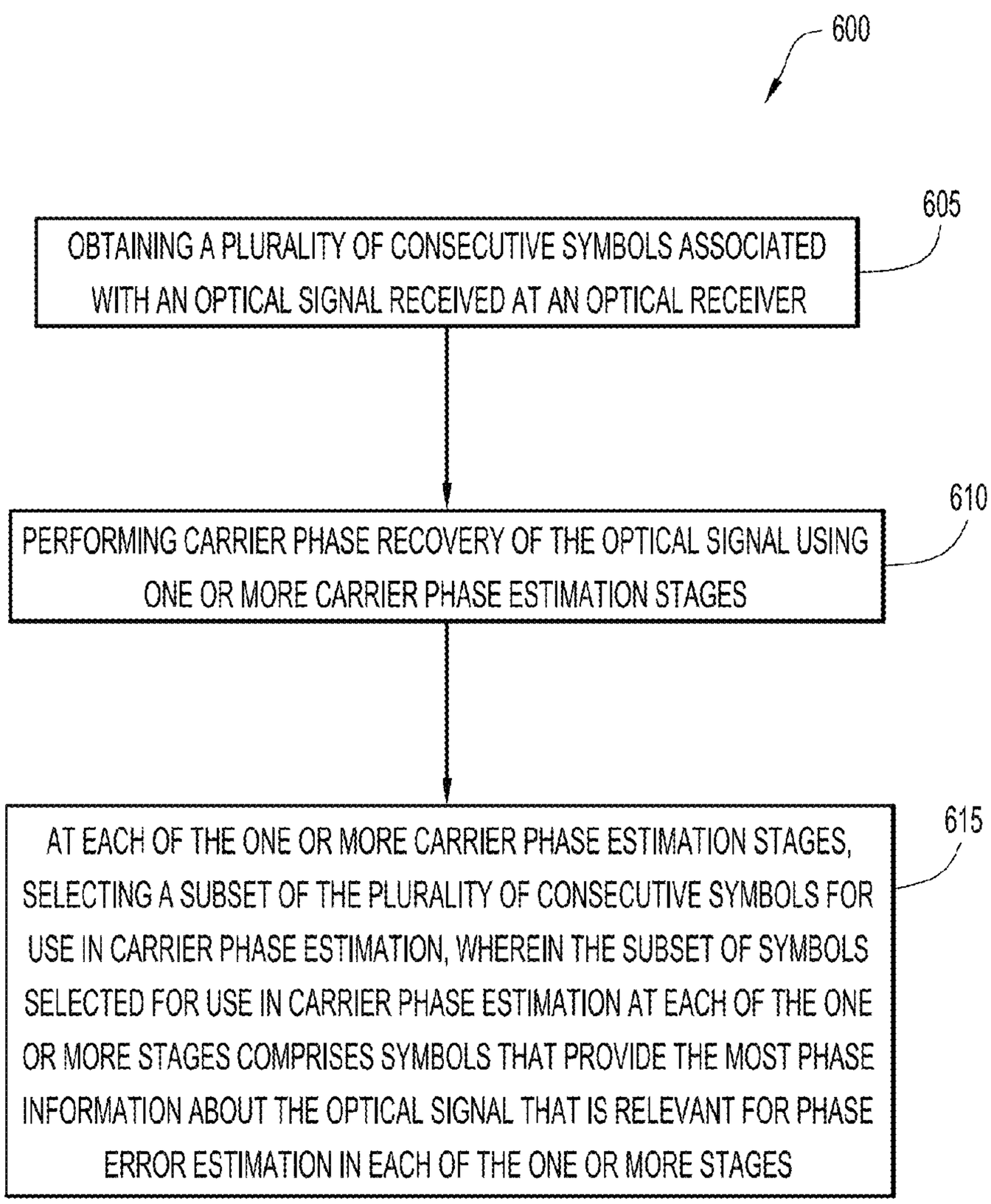
600
605
OBTAINING A PLURALITY OF CONSECUTIVE SYMBOLS ASSOCIATED WITH AN OPTICAL SIGNAL RECEIVED AT AN OPTICAL RECEIVER
610
PERFORMING CARRIER PHASE RECOVERY OF THE OPTICAL SIGNAL USING ONE OR MORE CARRIER PHASE ESTIMATION STAGES
615
AT EACH OF THE ONE OR MORE CARRIER PHASE ESTIMATION STAGES, SELECTING A SUBSET OF THE PLURALITY OF CONSECUTIVE SYMBOLS FOR USE IN CARRIER PHASE ESTIMATION, WHEREIN THE SUBSET OF SYMBOLS SELECTED FOR USE IN CARRIER PHASE ESTIMATION AT EACH OF THE ONE OR MORE STAGES COMPRISES SYMBOLS THAT PROVIDE THE MOST PHASE INFORMATION ABOUT THE OPTICAL SIGNAL THAT IS RELEVANT FOR PHASE ERROR ESTIMATION IN EACH OF THE ONE OR MORE STAGES

FIG.7

SUB-SAMPLED CARRIER PHASE RECOVERY

TECHNICAL FIELD

The present disclosure relates to carrier phase recovery in an optical receiver.

BACKGROUND

In recent years there has been an increase in the use of optical fiber communication networks. In an optical fiber communication network, an optical transmitter takes an electrical input and converts it to an optical output using a light source (e.g., laser diode, Light Emitting Diode (LED), etc.). The light from the transmitter is coupled into an optical fiber and is transmitted through the optical fiber to an optical receiver. The optical receiver converts the light back into an electrical signal.

Early optical fiber communication networks used transmission of one bit of information per data symbol. However, due to the need for high-capacity communications, there is an increasing demand for higher bit rates. This has led to the use of higher order modulation schemes for optical transmissions. Modulation schemes that have been implemented include, for example, Quaternary Phase Shift Keying (QPSK) and M-Quadrature Amplitude Modulation (M-QAM), wherein M is an integer with the power of 2 (i.e., 2, 4, 8, 16, 32, 64, etc.). In such modulation schemes, the optical transmitter includes an optical modulator that modulates the optical signal to carry the additional data.

BRIEF DESCRIPTION OF THE DRAWINGS

FIG. **1** is a block diagram of an optical receiver configured to execute sub-sampled carrier phase recovery techniques in accordance with examples presented herein.

FIG. **2**A is a schematic diagram of a parallelized Viterbi-Viterbi carrier phase estimation stage in accordance with examples presented herein.

FIG. **2**B is a schematic diagram illustrating sub-sampling and symbol selection logic in accordance with examples presented herein.

FIG. **3** is a schematic diagram illustrating ring partitioning in accordance with examples presented herein.

FIG. **4** is a schematic diagram of a two-stage carrier phase estimation with sub-sampled Viterbi-Viterbi and Maximum-Likelihood carrier phase estimation stages in accordance with examples presented herein.

FIG. **5** is a schematic diagram of another two-stage carrier phase estimation with sub-sampled Viterbi-Viterbi and Maximum-Likelihood carrier phase estimation stages in accordance with examples presented herein.

FIG. **6** is a schematic diagram of still another two-stage carrier phase estimation with sub-sampled Viterbi-Viterbi and Maximum-Likelihood carrier phase estimation stages in accordance with examples presented herein.

FIG. **7** is a flowchart of a sub-sampled carrier phase recovery technique in accordance with examples presented herein.

DESCRIPTION OF EXAMPLE EMBODIMENTS

Overview

Presented herein are sub-sampled carrier phase recovery techniques. In accordance with one example, a plurality of consecutive symbols associated with a received optical signal is obtained. Carrier phase recovery of the optical signal is performed using one or more carrier phase estimation stages. At each of the one or more carrier phase estimation stages, a subset of the plurality of consecutive symbols is selected for use in carrier phase estimation. The subset of symbols selected for use in carrier phase estimation at each of the one or more stages comprises symbols that provide the most phase information about the optical signal that is relevant for phase error estimation in each of the one or more stages.

EXAMPLE EMBODIMENTS

FIG. **1** is a block diagram illustrating part of a coherent optical receiver **10** configured to perform sub-sampled carrier phase recovery techniques in accordance with examples presented herein. The illustrated portion of optical receiver **10** comprises a chromatic dispersion (CD) filter module **12**, a polarization-mode dispersion (PMD) filter module **14**, a carrier phase recovery module **16**, and a Forward Error Correction (FEC) decoder **18**. The optical receiver **10** is a Polarization Multiplexed 16-Quadrature Amplitude Modulation (PM-16-QAM) optical receiver. That is, optical receiver **10** is configured to process and decode optical signals modulated in accordance with a modulation scheme that uses four in-phase (I) and four quadrature (Q) values that yield four bits per symbol, creating 16 possible states.

Complex-valued digital input data **20** is received and processed by the chromatic dispersion filter module **12** and the polarization-mode dispersion filter module **14**. As shown, the complex-valued digital input data **20** comprises X-polarized components in a scattered arrangement **22** and Y-polarized components in a scattered arrangement **23**. The chromatic dispersion filter module **12** may comprise one or more filters **21** for application to the X-polarized and Y-polarized components to compensate for the chromatic dispersion in the complex-valued digital input data **20**. Similarly, the polarization-mode dispersion filter module **14** may comprise one or more filters **30** for application to the X-polarized and Y-polarized components to compensate for the polarization-mode dispersion in the complex-valued digital input data **20**.

Filtered data **35** (i.e., data processed by the chromatic dispersion filter module **12** and the polarization-mode dispersion filter module **14**) is provided to the carrier phase recovery module **16**. The filtered data **35** includes X-polarized components in a ring-shaped pattern **24** and Y-polarized components in a ring-shaped pattern **25**.

The carrier phase recovery module **16** comprises two carrier phase estimation (CPE) blocks **40** each of which are associated with one of the X-polarized components and Y-polarized components. The X-polarized components and Y-polarized components may exchange phase estimation results to increase the overall estimation accuracy. The carrier phase estimation blocks **40** each comprise a Viterbi-Viterbi carrier phase estimation stage (Viterbi-Viterbi stage) **45** and a Maximum-Likelihood carrier phase estimation stage (Maximum-Likelihood stage) **50**. The Viterbi-Viterbi stages **45** each comprise Viterbi-Viterbi sub-sampling selection logic **55**, while the Maximum-Likelihood stages **50** each comprise Maximum-Likelihood sub-sampling selection logic **60**.

In general, phase error is induced by an optical channel and phase noise associated with the finite line width of the transmit laser and local-oscillator laser receiver. The carrier phase recovery module **16** is configured to estimate the phase error and use that phase error to generate phase recovered data **65**. That is, the carrier phase recovery module **16** is configured to use the estimated phase error to convert the ring shaped patterns **24** and **25** in the filtered data **35** to respective 16-QAM constellations (i.e. constellations from which the phase error

has been removed) **26** and **27**. FIG. **1** illustrates the standard 16-QAM constellations **26** (corresponding to the X-polarized components) and **27** (corresponding to the Y-polarized components) forming part of the phase-recovered data **65**. The phase-recovered data **65** is provided to Forward Error Correction (FEC) decoder **18**.

Certain conventional techniques perform carrier phase estimation based on all received symbols. These conventional methods are accurate and provide good tolerance to laser phase noise, non-linear phase noise, and local oscillator (LO)-frequency offset. However, these methods are also complex and may consume significant amounts of power. Presented herein are techniques that select a subset of symbols for use in one or more carrier phase estimation stages in order to reduce the power requirements associated with the carrier phase recovery. The techniques presented herein select the subset of symbols in a manner that substantially maintains a high level performance achieved with techniques that use all received symbols for carrier phase recovery.

More specifically, as described further below, the carrier phase estimation blocks **40** of FIG. **1** are configured to implement sub-sampling selection techniques in which only certain symbols (i.e., a subset of the received symbols) are used during carrier phase recovery (e.g., in each of the Viterbi-Viterbi carrier phase estimation stages **45** and the Maximum-Likelihood carrier phase estimation stages **50**). The symbols selected for use in each stage are, in general, the symbols with the highest ratio between the measured signal phase error and additive noise. That is, the symbols that provide the most phase information about the received optical signal that is relevant for a specific stage are selected for use in that stage. The "most phase information about the received optical signal that is relevant for a specific stage" refers to the most available phase recovery information for a given stage. For instance, the Viterbi-Viterbi carrier phase estimation is unable to use constellation points in the 2^{nd} ring, whilst constellation points in the outer rings give the minimum phase error for a given amount of additive noise.

Reference is now made to FIGS. **2**A, **2**B, and **3**. FIG. **2**A is a schematic diagram illustrating sub-sampling selection techniques in an example Viterbi-Viterbi carrier phase estimation stage **45** in accordance with examples presented herein. As shown, the Viterbi-Viterbi stage **45** comprises a ring partitioning segment **80**, the aforementioned sub-sampling selection logic **55**, a 4^{th}-power function segment **85**, an adder tree segment **90** (for moving average filtering), an unwrapping segment **95** (vector-to-angle conversion, unwrapping, phase-to-vector conversion), and a symbol rotation segment **100**.

In operation, optical signals are received at an optical receiver at a high rate (e.g., at a rate of 32 giga-baud (GBAUD), but the application-specific integrated circuit (ASIC) of the optical receiver and/or other hardware components are typically clocked at a lower rate (e.g., they operate with a 500 Megahertz (MHz) clock). Therefore, the Viterbi-Viterbi stage **45** operates on a plurality of symbols in parallel. In the example of FIG. **2**A, 16 symbols are received and processed in parallel and are referred to as symbols R**1** through R**16**. It is to be appreciated that the use of 16 symbols is merely illustrative and that different numbers of symbols (e.g., 12, 32, 96, 108, etc.) could be processed in parallel, depending on the capabilities of the ASIC and/or other hardware components.

The parallel processing of a plurality (e.g., 16) of symbols through the entire Viterbi-Viterbi stage **45** may consume significant power. The sub-sampling selection techniques presented herein reduce the number of symbols processed at various segments of the Viterbi-Viterbi stage **45**, thereby reducing the power consumed by the Viterbi-Viterbi stage **45**.

A 4^{th}-power function is an operation applicable to Quaternary Phase Shift Keying (QPSK) signals for phase error estimation. The 4^{th}-power function segment **85** is used to remove the QPSK signals, thereby leaving only the phase error and additive noise. That is, the 4^{th}-power function segment **85** generates a vector from which the data has been removed. For 16-QAM the 4^{th}-power function cannot be directly applied in the same way as with QPSK signals. Therefore, a so-called "ring partitioning" approach is used in which, as shown in FIG. **3**, a 16-QAM constellation is generally divided into three rings, namely a first (inner) ring **110**, a second (middle) ring **115**, and a third (outer) ring **120**. The rings, sometimes referred to herein as constellation radius rings, are used to group constellation points (symbols) into classes based on their distance from the center of the constellation.

More specifically, the first ring **110** is set a first distance from the center of the constellation (i.e., the first ring has a first radius representing the distance from the center of the constellation to the first ring). A number of symbols positioned less than this first distance from the center of the constellation will fall within the first ring **110**. The second ring **115** is set a second distance from the center of the constellation (i.e., the second ring has a second radius representing the distance from the center to the second ring). A number of symbols positioned less than the second distance from the center of the constellation, but greater than the first distance will fall within the second ring **115**. The third ring **120** is set a third distance from the center of the constellation (i.e., the third ring has a third radius representing the distance from the center to the third ring). A number of symbols positioned less than the third distance from the center of the constellation, but greater than the second distance will fall within the third ring **120**.

The first ring **110** and the third ring **120** are both QPSK-like because they each include four symbol points. The second ring **115** is not QPSK-like because it includes eight symbol points (with unequal angular spacing). In the example configuration of the Viterbi-Viterbi stage of FIG. **2**A, the ring partitioning is performed on the 16 received (original) symbols R**1** through R**16** at ring partitioning segment **80**. That is, when a symbol is received, the ring partitioning segment **80** determines within which of the three rings **110**, **115**, or **120** the symbol falls.

As noted above, symbols R**1** through R**16** are received at ring partitioning segment **80**. FIG. **2**A illustrates, in ring partitioning segment **80**, one box corresponding to each of these received symbols R**1** through R**16** that includes a number "1", "2", or "3" therein. The number within the box indicates the ring to which the received symbol belongs. For example, symbol R**1** is associated with a box that includes the number "3" therein, indicating that symbol R**1** falls in the third ring **120** (i.e., the ring partitioning segment **80** has classified symbol R**1** as a member of the third ring **120**). Symbols R**2** and R**3** are associated with boxes that include the number "2," indicating that symbols R**2** and R**3** fall within the second ring **115**; symbol R**4** is associated with a box that includes the number "1," indicating that symbol R**4** falls within the first ring **110**; and so on. Table 1, below, illustrates the received symbols of FIG. **2**A and within which ring each of those symbols fall.

TABLE 1

Symbol	Ring
Symbol R1	Third Ring
Symbol R2	Second Ring
Symbol R3	Second Ring
Symbol R4	First Ring
Symbol R5	Second Ring
Symbol R6	Third Ring
Symbol R7	First Ring
Symbol R8	Third Ring
Symbol R9	Second Ring
Symbol R10	Second Ring
Symbol R11	Second Ring
Symbol R12	Third Ring
Symbol R13	Second Ring
Symbol R14	First Ring
Symbol R15	Second Ring
Symbol R16	Third Ring

The sub-sampling selection logic **55** is connected between the ring partitioning segment **80** and the 4^{th}-power function segment **85**. The sub-sampling selection logic **55** is configured to select a subset of the received symbols R**1** through R**16** for processing by the subsequent segments in the Viterbi-Viterbi stage **45**. In general, the symbols selected for subsequent use are the symbols that provide the most phase information about the optical signal that is relevant for phase error estimation in the subsequent Viterbi-Viterbi operations. More specifically, the 4^{th}-power function results in a vector of the phase of a symbol. Additive Gaussian noise on a symbol will cause a greater phase error for symbols which fall within lower rings. Therefore phase estimates from symbols in outer rings have more valuable information than those in inner rings and should be selected preferentially. In addition, the 4^{th} power operation results in a longer vector for outer rings and hence weights those phase estimations preferentially. Other techniques involve normalizing the 4^{th} power vectors so that all are of the same length, and then applying a scaling (e.g. ×2, ×3, ×4) afterwards. The 4^{th}-power function may only be used with symbols that fall within the first ring **110** or the third ring **120** (i.e., cannot be applied to second ring symbols). As such, with regards to the application of the 4^{th}-power function to received symbols, the most phase information about the optical signal that is relevant for phase error estimation in a Viterbi-Viterbi stage can be obtained using third ring symbols, while the second most phase information for phase error estimation in a Viterbi-Viterbi stage can be obtained using first ring symbols, and no information can be obtained from second ring symbols.

In the example of FIG. **2**A, the 16 received symbols R**1** through R**16** are organized (divided) into eight (8) groups **130**(**1**)-**130**(**8**) that each comprises two sequential symbols (i.e. pairs of symbols). For example, group **130**(**1**) includes symbols R**1** and R**2**, group **130**(**2**) includes symbols R**3** and R**4**, and so on. As such, FIG. **2**A illustrates a sub-sampling factor of 2 that has approximately half of the complexity of a conventional approach that processes all parallel symbols. The sub-sampling logic **55** is configured to evaluate the symbols within a group to select the symbol in that group that, when the 4^{th}-power function is applied thereto, will provide the most phase information about the optical signal that is relevant for phase error estimation in a Viterbi-Viterbi stage (i.e., identify the symbol with the highest ratio between the measured signal phase error and additive noise and which is useable in the Viterbi-Viterbi stage. For example, as noted, group **130**(**1**) comprises symbols R**1** and R**2**. R**1** falls within the third ring **120**, while R**2** falls within the second ring **115**. Third ring symbols provide the most information for phase error correction (i.e., have the highest ratio between the measured signal phase error and additive noise). Second ring symbols have the second highest ratio between the measured signal phase error and additive noise, but cannot be used with the 4^{th}-power function and thus do not provide any information for phase error correction in the Viterbi-Viterbi stage **45**. As such, from group **130**(**1**) symbol R**1** is selected for subsequent processing by the 4^{th}-power function segment **85**, while symbol R**2** is discarded (i.e., omitted for use in processing by the 4^{th}-power function segment **85**).

As a further example, group **130**(**4**) comprises symbols R**7** and R**8**. R**7** falls within the first ring **110**, while R**8** falls within the third ring **120**. Third ring symbols have the highest ratio between the measured signal phase error and additive noise, while first ring symbols have the lowest ratio between the measured signal phase error and additive noise. As such, from group **130**(**4**), symbol R**8** is selected for subsequent processing by the 4^{th}-power function segment **85**, while symbol R**7** is discarded.

Furthermore, group **130**(**5**) comprises symbols R**9** and R**10** that both fall within the second ring **115**. As noted, second ring symbols cannot be used with the 4^{th}-power function and thus do not provide any information for phase error correction in the Viterbi-Viterbi stage **45**. As such, no symbols from group **130**(**5**) are selected for subsequent processing by the 4^{th}-power function segment **85**. That is, both symbols R**9** and R**10** are discarded.

The symbols that are selected from each group **130**(**1**)-**130**(**8**) are circled in FIG. **2**A. Additionally, Table 2 below illustrates each of the groups **130**(**1**)-**130**(**8**), the symbols in each group, the symbol that is selected for subsequent Viterbi-Viterbi stage operations, and the selected symbol ring classification.

Group	First Group Member	Second Group Member	Selected Symbol	Selected Symbol Ring
130(1)	Symbol R1	Symbol R2	Symbol R1	Ring 3
130(2)	Symbol R3	Symbol R4	Symbol R4	Ring 1
130(3)	Symbol R5	Symbol R6	Symbol R6	Ring 3
130(4)	Symbol R7	Symbol R8	Symbol R8	Ring 3
130(5)	Symbol R9	Symbol R10	None	None
130(6)	Symbol R11	Symbol R12	Symbol R12	Ring 3
130(7)	Symbol R13	Symbol R14	Symbol R14	Ring 1
130(8)	Symbol R15	Symbol R14	Symbol R16	Ring 3

As noted above, the ring partitioning segment **80** determines within which ring a received symbol falls. The sub-sampling selection logic **55** comprises one or more hardware elements (e.g., switches, multiplexers, etc.) that use the ring partitioning segment information to select the appropriate symbols. Further details of the sub-sampling and symbol selection logic **55** are provided below with reference to FIG. **2**B. In essence, the sub-sampling selection logic **55** is configured to perform a comparison of the symbols within a group **130**(**1**)-**130**(**8**) to determine which one has the highest relative ratio between the measured signal phase error and additive noise and is useable for phase error estimation in the subsequent Viterbi-Viterbi operations.

FIG. **2**A illustrates an example in which the groups **130**(**1**)-**130**(**8**) each have two members and where one symbol is selected from each group. It is to be appreciated that these examples are merely illustrative and that other group sizes (e.g., groups of 4 symbols) are possible.

In the example of FIG. **2**A, as a result of the sub-sampling selection logic **55**, seven symbols are selected for processing by the 4^{th}-power function segment **85**. As noted, the 4^{th}-

power function segment **85** produces vectors from which the original data has been removed. These vectors are then provided to the adder tree segment **90**.

Each of the received symbols has some noise associated therewith. The adder tree segment **90** is configured to use the vectors provided by the 4^{th}-power function segment **85** to generate, for each group **130(1)-130(8)**, an averaged vector over a sliding/moving window. This process reduces noise in the vectors.

It should be noted that the group **130(5)** associated with R**9** and R**10** does not provide any symbol to the 4^{th}-power function segment **85**. Accordingly, the 4^{th}-power function segment **85** does not provide a vector to the adder tree segment **90**. However, due to the averaging function of the adder tree segment **90**, an output for group **130(5)** is still produced (using the surrounding vectors) by the adder tree segment **90** that may be used for subsequent processing.

The averaged vectors for groups **130(1)-130(8)** produced by adder tree segment **90** are provided to the unwrap segment **95** to remove occasional phase jumps because of the 90 degree phase ambiguity (4^{th} power function). Using the averaged vectors, the unwrapping segment **95** generates a Viterbi-Viterbi estimated phase correction (offset) **132(1)-132(8)** for each group. At the symbol rotation segment **100**, the Viterbi-Viterbi estimated phase corrections **132(1)-132(8)** are then applied to the original symbols in the respective group.

More specifically, at the symbol rotation segment **100**, each of the original symbols R**1** through R**16** are provided to an associated processing block **135(1)-135(16)**. Each block also receives a Viterbi-Viterbi stage phase error correction for the corresponding group. For example, blocks **135(1)** and **135(2)** receive the original symbols R**1** and R**2**, respectively. The blocks **135(1)** and **135(2)** also receive the Viterbi-Viterbi stage phase error correction **132(1)** corresponding to group **130(1)** to which symbols R**1** and R**2** belong. That is, the Viterbi-Viterbi stage phase error correction **132(1)** generated from R**1** is used for the phase error correction of both symbols R**1** and R**2** at the symbol rotation segment **100**. Table 3, below, illustrates the Viterbi-Viterbi stage phase error correction signal that is used to correct each of the symbols R**1** through R**16** at the symbol rotation segment **100**.

TABLE 3

Symbol	Correction Signal
Symbol R1	132(1)
Symbol R2	132(1)
Symbol R3	132(2)
Symbol R4	132(2)
Symbol R5	132(3)
Symbol R6	132(3)
Symbol R7	132(4)
Symbol R8	132(4)
Symbol R9	132(5)
Symbol R10	132(5)
Symbol R11	132(6)
Symbol R12	132(6)
Symbol R13	132(7)
Symbol R14	132(7)
Symbol R15	132(8)
Symbol R16	132(8)

The symbol rotation segment **100** is configured to output a plurality of Viterbi-Viterbi phase error corrected signals, shown in FIG. **2**A as symbols R**1'** though R**16'**. These symbols R**1'** through R**16'** may then be provided to the Maximum-Likelihood stage **50** of the phase error correction module **40** for additional phase correction, as described further below.

It should be noted that if the subsequent Maximum-Likelihood stage **50** is also sub-sampled, it is sufficient to apply the symbol rotation segment only to those symbols that will be used in the Maximum-Likelihood stage **50**. This further reduces complexity and power dissipation.

As noted, FIG. **2**B is a schematic diagram illustrating further details of the sub-sampling selection logic **55** and ring portioning segment **80**. As shown, symbols R**1** through R**16** are received and provided to the ring portioning segment **80** and a timing segment **57**. The ring portioning segment **80** includes a vector length calculation block **81** that feeds a ring decision block **82**. The output from the ring decision block **82** is provided to selection block **58**. The sub-sampling selection logic **55** also comprises a multiplexer **59** connected to the timing block **57** and the selection block **58** that uses the signals from these blocks to generate an output (X_{select}) representing the selected symbol for a group of symbols.

FIG. **4** is a schematic diagram illustrating sub-sampling selection techniques in an example Maximum-Likelihood stage **250** connected to a Viterbi-Viterbi stage **245**. As noted above, optical signals are received at an optical receiver at a high rate (e.g., at a rate of 32 GBAUD, but the receiver ASIC and/or other hardware components are typically clocked at a lower rate (e.g., they operate with a 500 MHz clock). Therefore, the Viterbi-Viterbi stage **245** and Maximum-Likelihood stage **250** operate on a plurality of symbols in parallel. In the example of FIG. **4**, 12 symbols are received and processed in parallel and are referred to as received (original) symbols R**1** through R**12**. It is to be appreciated that the use of 12 symbols is merely illustrative and that different numbers of symbols (e.g., 12, 32, 96, 108, etc.) could be processed in parallel, depending on the capabilities of the ASIC and/or other hardware components.

The parallel processing of a plurality (e.g., 12) symbols through the Viterbi-Viterbi stage **245** and Maximum-Likelihood stage **250** may consume significant power. The sub-sampling selection techniques presented herein reduce the number of symbols processed at various segments of both the Viterbi-Viterbi stage **245** and the Maximum-Likelihood stage **250**, thereby reducing the power consumed at the optical receiver.

In the example of FIG. **4**, the Viterbi-Viterbi stage **245** operates substantially the same as described above with reference to FIG. **2**A to generate a plurality of Viterbi-Viterbi phase error corrected signals, shown in FIG. **4** as symbols R**1'** though R**12'**. More specifically, the Viterbi-Viterbi stage **245** includes a ring partitioning segment **280** configured to determine within which of the three rings **110**, **115**, or **120** (as shown in FIG. **3**) each of the received symbols R**1** through R**12** falls. FIG. **4** illustrates, in ring partitioning segment **280**, one box corresponding to each of the received symbols that includes a number "1", "2", or "3" therein. The number within the box indicates the ring to which the received symbol belongs. Table 4, below, illustrates the received symbols R**1** through R**12** of FIG. **4** and which ring each of those symbols fall within.

TABLE 4

Symbol	Ring
Symbol R1	Third Ring
Symbol R2	Second Ring
Symbol R3	Second Ring
Symbol R4	First Ring
Symbol R5	Second Ring
Symbol R6	First Ring
Symbol R7	Second Ring

TABLE 4-continued

Symbol	Ring
Symbol R8	First Ring
Symbol R9	Second Ring
Symbol R10	Third Ring
Symbol R11	Third Ring
Symbol R12	First Ring

As shown, sub-sampling selection logic **255** is connected between the ring partitioning segment **280** and a sub-sampled Viterbi-Viterbi phase estimation and correction block **205**. The sub-sampling selection logic **255** is, similar to the sub-sampling logic **55** of FIG. **2**A, configured to select a subset of the received symbols R**1** through R**12** for processing by the subsequent segments in the Viterbi-Viterbi stage **245**. In general, the symbols selected for subsequent use are the symbols that provide the most phase information about the optical signal that is relevant for phase error estimation in the subsequent Viterbi-Viterbi operations.

More specifically, as noted above, the 4^{th}-power function results in a vector of the phase of a symbol. Additive Gaussian noise on a symbol will cause a greater phase error for symbols which fall within lower rings. Therefore phase estimates from symbols in outer rings have more valuable information than those in inner rings and should be selected preferentially. In addition, the 4^{th} power operation results in a longer vector for outer rings and hence weights those phase estimations preferentially. Other techniques involve normalizing the 4^{th} power vectors so that all are of the same length, and then applying a scaling (e.g. ×2, ×3, ×4) afterwards. The 4^{th}-power function may only be used with symbols that fall within the first ring **110** or the third ring **120** (i.e., cannot be applied to second ring symbols). As such, with regards to the application of the 4^{th}-power function to received symbols, the most phase information about the optical signal that is relevant for phase error estimation in a Viterbi-Viterbi stage can be obtained using third ring symbols, while the second most phase information for phase error estimation in a Viterbi-Viterbi stage can be obtained using first ring symbols, and no information can be obtained from second ring symbols.

In the example of FIG. **4**, the 12 received symbols R**1** through R**12** are divided into three (3) groups **220**(**1**), **220**(**2**), and **220**(**3**) that each comprises four sequential symbols. For example, group **220**(**1**) includes symbols R**1**-R**4**, group **220**(**2**) includes symbols R**5**-R**8**, and group **220**(**3**) includes symbols R**9**-R**12**. The sub-sampling logic **255** is configured to evaluate the symbols within each of the groups **220**(**1**)-**220**(**3**) to select the symbol in that group that, when the 4^{th}-power function is applied thereto, will provide the most information for phase error correction. The symbols that are selected from each group **220**(**1**), **220**(**2**), and **220**(**3**) are circled in FIG. **4**. Additionally, Table 5 below illustrates each of the groups **220**(**1**), **220**(**2**), and **220**(**3**); the symbols in each group, the symbol that is selected for subsequent Viterbi-Viterbi stage operations, and the selected symbol ring classification.

TABLE 5

Group	First Group Member	Second Group Member	Third Group Member	Fourth Group Member	Selected Symbol	Selected Symbol Ring
220(1)	Symbol R1	Symbol R2	Symbol R3	Symbol R4	Symbol R1	Ring 3
220(2)	Symbol R5	Symbol R6	Symbol R7	Symbol R8	Symbol R6	Ring 1
220(3)	Symbol R9	Symbol R10	Symbol R11	Symbol R12	Symbol R10	Ring 3

The sub-sampled Viterbi-Viterbi phase estimation and correction block **205** represents the operations/functions that are performed to generate Viterbi-Viterbi phase error corrected signals, shown in FIG. **4** as symbols R**1'** though R**12'**. In this example, the sub-sampled Viterbi-Viterbi phase estimation and correction block **205** corresponds to the 4^{th}-power function operations, the adder tree operations, the unwrapping operations, and the symbol rotation operations described above. As noted elsewhere herein, in certain examples only symbols that will used for the sub-sampled Maximum-Likelihood stage **250** are rotated before the Maximum-Likelihood stage **250** to reduce complexity.

As a result of the processing described above, the plurality of Viterbi-Viterbi phase error corrected symbols R**1'** though R**12'** (or a subset thereof) are provided to the Maximum-Likelihood stage **250**. The Maximum-Likelihood stage **250** comprises sub-sampling selection logic **225**, a sub-sampled Maximum-Likelihood phase estimation block **226**, and a symbol rotation segment **234**.

Sub-sampling selection logic **225** is configured to receive the Viterbi-Viterbi phase error corrected symbols R**1'** though R**12'** and is configured to select a subset of these symbols R**1'** through R**12'** for processing by the subsequent segments in the Maximum-Likelihood stage **250**. The sub-sampling selection logic **225** may be implemented in a manner similar to the arrangement of FIG. **2**B. In general, the symbols selected for subsequent use are the symbols that provide the most phase information about the optical signal that is relevant for the subsequent Maximum-Likelihood operations. More specifically, depending on the constellation symbol a certain phase error (angle) translates into error vectors with varying length. First ring symbols translate into the shortest length vector, second ring symbols translate into a medium length vector, and third ring symbols translate into the longest vector. The Additive white Gaussian noise that impairs the phase error estimation is independent of the constellation symbol. Consequently, the ratio between the measured signal phase error and additive white Gaussian noise varies with the diameter of each ring, where first ring symbols provide a weak phase estimate, second ring symbols provide a medium phase estimate, and third ring symbols provide a strong phase estimate. In other words, outer constellations have better phase information.

In the example of FIG. **4**, the 12 Viterbi-Viterbi phase error corrected symbols R**1'** though R**12'** are divided into six (6) groups **230**(**1**)-**230**(**6**) that each comprise two sequential symbols (i.e., symbol pairs). For example, group **230**(**1**) includes symbols R**1'** and R**2'**, group **230**(**2**) includes symbols R**3'** and R**4'**, and so on. The sub-sampling logic **225** is configured to evaluate the symbols within a group to select the symbol in that group that will provide the most phase information about the optical signal that is relevant for the subsequent Maximum-Likelihood operations (i.e., the symbol having the highest ratio between the measured signal phase error and additive noise). For example, as noted previously, group **230**(**1**) com-

prises symbols R1' and R2'. R1' falls within the third ring **120**, while R2' falls within the second ring **115**. Third ring symbols have the highest ratio between the measured signal phase error and additive noise, while second ring symbols have the second highest ratio between the measured signal phase error and additive noise. As such, symbol R1' is selected from group **230**(**1**) for subsequent processing, while symbol R2' is discarded (i.e., omitted for use in processing by the sub-sampled Maximum-Likelihood phase estimation block **226**).

As a further example, group **230**(**2**) comprises symbols R3' and R4'. R3' falls within the second ring **115**, while R4' falls within the third ring **120**. Second ring symbols have the second highest ratio between the measured signal phase error and additive noise, while first ring symbols have the lowest ratio between the measured signal phase error and additive noise. As such, from group **230**(**2**) symbol R3' is selected for subsequent processing, while symbol R4' is discarded.

The symbols that are selected from each group **230**(**1**)-**230**(**6**) are circled in FIG. **4**. Additionally, Table 6 below illustrates each of the groups **230**(**1**)-**230**(**6**), the symbols in each group, and the symbol that is selected for subsequent Maximum-Likelihood stage operations, and the selected symbol ring classification.

TABLE 6

Group	First Group Member	Second Group Member	Selected Symbol	Selected Symbol Ring
230(1)	Symbol R1'	Symbol R2'	Symbol R1'	Ring 3
230(2)	Symbol R3'	Symbol R4'	Symbol R3'	Ring 2
230(3)	Symbol R5'	Symbol R6'	Symbol R5'	Ring 2
230(4)	Symbol R7'	Symbol R8'	Symbol R7'	Ring 2
230(5)	Symbol R9'	Symbol R10'	Symbol R10'	Ring 3
230(6)	Symbol R11'	Symbol R12'	Symbol R11'	Ring 3

The sub-sampling selection logic **225** comprises one or more hardware elements (e.g., switches, multiplexers, etc.) that use the ring partitioning segment information to select the appropriate symbols. In essence, the sub-sampling selection logic **225** is configured to perform a comparison of the symbols within a group **230**(**1**)-**230**(**6**) to determine which one has the relative highest ratio between the measured signal phase error and additive noise. If both the Viterbi-Viterbi and Maximum-Likelihood stages are sub-sampled, the vector-length and ring decisions do not need to be made again within the sub-sampling logic **225** (as they were already completed in sub-sampling logic **255**). In such examples, only the symbol selection block changes.

FIG. **4** illustrates an example in which the groups **230**(**1**)-**230**(**6**) each have two members and where one symbol is selected from each group. It is to be appreciated that these examples are merely illustrative and that other group sizes (e.g., groups of 4 symbols) are possible.

In the example of FIG. **4**, as a result of the sub-sampling selection logic **225**, six symbols are selected for processing by the sub-sampled Maximum-Likelihood phase estimation block **226**. In general, the sub-sampled Maximum-Likelihood phase estimation block **226** is configured to perform Maximum-Likelihood operations using the six selected symbols (symbols R1', R3', R5', R7', R10', and R11') to generate a Maximum-Likelihood phase estimates (offset) **232**(**1**)-**232**(**6**) for each group. Details of an example Maximum-Likelihood phase estimation block are provided below with reference to FIG. **6**.

At the symbol rotation segment **235**, the Maximum-Likelihood phase estimates **232**(**1**)-**232**(**6**) are applied to the Viterbi-Viterbi phase error corrected symbols R1' though R12' in the respective group. More specifically, at the symbol rotation segment **235**, each of the Viterbi-Viterbi phase error corrected symbols R1' though R12' are provided to an associated processing block **235**(**1**)-**235**(**12**). Each block **235**(**1**)-**235**(**12**) also receives a Maximum-Likelihood phase estimate for the corresponding group. For example, blocks **235**(**1**) and **235**(**2**) receive the Viterbi-Viterbi phase error corrected symbols R1' and R2', respectively. The blocks **235**(**1**) and **235**(**2**) also receive the Maximum-Likelihood phase estimate **232**(**1**) corresponding to group **230**(**1**) to which symbols R1' and R2' belong. That is, the Maximum-Likelihood phase estimate **232**(**1**) generated from R1' is used for the phase error correction of both symbols R1' and R2' at the symbol rotation segment **235**. Table 7 below illustrates the Maximum-Likelihood phase estimate that is used to correct each of the symbols R1' through R12' at the symbol rotation segment **235**.

TABLE 7

Symbol	Correction Signal
Symbol R1'	232(1)
Symbol R2'	232(1)
Symbol R3'	232(2)
Symbol R4'	232(2)
Symbol R5'	232(3)
Symbol R6'	232(3)
Symbol R7'	232(4)
Symbol R8'	232(4)
Symbol R9'	232(5)
Symbol R10'	232(5)
Symbol R11'	232(6)
Symbol R12'	232(6)

In certain embodiments, to reduce the overall complexity of the two stage carrier recovery, the Viterbi-Viterbi phase estimate is only applied to symbols that will be considered in the Maximum-Likelihood stage (R1', R3', R5', R7', R10' and R11') behind the Viterbi-Viterbi stage. And after Maximum-Likelihood phase error estimation the sum of the Viterbi-Viterbi estimate and the Maximum-Likelihood estimate is applied to all corresponding uncorrected symbols (R1-R12). Such an arrangement is shown below in FIG. **6**.

The symbol rotation segment **235** is configured to output a plurality of complete phase error corrected signals, shown in FIG. **4** as symbols R1" though R12". These symbols R1" through R12" represent fully phase recovered symbols (i.e., symbols that have undergone both Viterbi-Viterbi and Maximum-Likelihood phase error recovery). The fully phase recovered symbols may be provided to a Forward Error Correction decoder for subsequent processing.

FIG. **5** is a schematic diagram illustrating alternative sub-sampling selection techniques in a Maximum-Likelihood stage **350** connected to Viterbi-Viterbi stage **245**. Viterbi-Viterbi stage **245** operates as described above with reference to FIG. **4** to generate the plurality of Viterbi-Viterbi phase error corrected symbol R1' though R12'. As a result, the plurality of Viterbi-Viterbi phase error corrected symbols R1' though R12' are provided to the Maximum-Likelihood stage **350**. The Maximum-Likelihood stage **350** comprises sub-sampling selection logic **325**, a sub-sampled Maximum-Likelihood phase estimation block **326**, and a symbol rotation segment **334**.

Similar to sub-sampling selection logic **225** of FIG. **4**, the sub-sampling selection logic **325** is configured to select a subset of the received symbols R1' through R12' for processing by the subsequent segments in the Maximum-Likelihood stage **350**. In general, the symbols selected for subsequent use are the symbols that have the highest ratio between the mea-

sured signal phase error and additive noise. However, in addition to selecting the symbols that have the highest ratio between the measured signal phase error and additive noise, the sub-sampling selection logic **325** is also configured to only select symbols for which a precursor to that symbol was not used in the Viterbi-Viterbi stage operations. In other words, if a symbol is used in the Viterbi-Viterbi stage **245**, the sub-sampling selection logic **325** is configured to eliminate the Viterbi-Viterbi phase error corrected version of that symbol for use in the Maximum-Likelihood stage **350**. In essence, the sub-sampling selection logic **325** performs a two-stage selection process that eliminates Viterbi-Viterbi phase error corrected versions of symbols used in the Viterbi-Viterbi stage **245** and that, from the remaining symbols, selects the one that has the highest ratio between the measured signal phase error and additive noise. This guarantees maximum utilization of the available information about the actual phase error, since the previously unused symbols will contain the phase-error and an uncorrelated noise component which can be averaged.

In the example of FIG. **5**, the 12 Viterbi-Viterbi phase error corrected symbols R**1**' though R**12**' are divided into six (6) groups **330**(**1**)-**330**(**6**). The groups **330**(**1**)-**330**(**6**) in this each comprise two sequential symbols (i.e., a pair of symbols). For example, group **330**(**1**) includes symbols R**1**' and R**2**', group **330**(**2**) includes symbols R**3**' and R**4**', and so on.

As noted, the sub-sampling logic **325** performs a two-stage selection process to evaluate the symbols within a group to select a symbol in that group that will provide the most phase information about the optical signal that is relevant for phase error estimation in the subsequent Maximum-Likelihood operations. For example, group **330**(**1**) comprises Viterbi-Viterbi phase error corrected signals symbols R**1**' and R**2**'. R**1**' falls within the third ring **120**, while R**2**' falls within the second ring **115**. Again, third ring symbols have the highest ratio between the measured signal phase error and additive noise, while second ring symbols have the second highest ratio between the measured signal phase error and additive noise. However, symbol R**1** (the precursor to symbol R**1**') was selected from group **220**(**1**) in the Viterbi-Viterbi stage **245**. As such, sub-sampling selection logic **325** eliminates symbol R**1**' from use in the Maximum-Likelihood stage **350**. Accordingly, sub-sampling selection logic **325** selects symbol R**2**' for subsequent processing.

As a further example, group **330**(**2**) comprises symbols R**3**' and R**4**'. R**3**' falls within the second ring **115**, while R**4**' falls within the third ring **120**. Neither of the precursors for symbols R**3**' or R**4**' (i.e., symbols R**3** or R**4**) were used in the Viterbi-Viterbi stage. As such, since second ring symbols have the second highest ratio between the measured signal phase error and additive noise, while first ring symbols have the lowest ratio between the measured signal phase error and additive noise, symbol R**3**' is selected from group **330**(**2**) for subsequent processing and symbol R**4**' is discarded.

In another example, group **330**(**5**) comprises symbols R**9**' and R**10**'. R**9**' falls within the second ring **115**, while R**20**' falls within the third ring **110**. Third ring symbols have the highest ratio between the measured signal phase error and additive noise, while second ring symbols have the second highest ratio between the measured signal phase error and additive noise. However, symbol R**10** (the precursor to symbol R**10**') was selected from group **220**(**3**) in the Viterbi-Viterbi stage **245**. As such, sub-sampling selection logic **325** eliminates symbol R**10**' from use in the Maximum-Likelihood stage **350**. Accordingly, sub-sampling selection logic **325** selects symbol R**9**' for subsequent processing.

The symbols that are selected from each group **330**(**1**)-**330**(**6**) are circled in FIG. **5**. Additionally, Table 8 below illustrates each of the groups **330**(**1**)-**330**(**6**), the symbols in each group, the symbol that is selected for subsequent Maximum-Likelihood stage operations, and the selected symbol ring classification.

TABLE 8

Group	First Group Member	Second Group Member	Selected Symbol	Selected Symbol Ring
330(1)	Symbol R1'	Symbol R2'	Symbol R2'	Ring 2
330(2)	Symbol R3'	Symbol R4'	Symbol R3'	Ring 2
330(3)	Symbol R5'	Symbol R6'	Symbol R5'	Ring 2
330(4)	Symbol R7'	Symbol R8'	Symbol R7'	Ring 2
330(5)	Symbol R9'	Symbol R10'	Symbol R9'	Ring 2
330(6)	Symbol R11'	Symbol R12'	Symbol R11'	Ring 3

The sub-sampling selection logic **325** comprises one or more hardware elements (e.g., switches, multiplexers, etc.) that use the ring partitioning segment information to select the appropriate symbols. In essence, the sub-sampling selection logic **325** is configured to perform a two-stage analysis of the symbols within a group **330**(**1**)-**330**(**6**). First, the sub-sampling selection logic **325** eliminates any symbols for which a precursor of the symbols was used in the Viterbi-Viterbi stage **245**. Second, the sub-sampling selection logic **325** selects, from any remaining symbols, the symbol that have the highest ratio between the measured signal phase error and additive noise.

FIG. **5** illustrates an example in which the groups **330**(**1**)-**330**(**6**) each have two members and where one symbol is selected from each group. It is to be appreciated that these examples are merely illustrative and that other group sizes (e.g., groups of 4 symbols) are possible.

In the example of FIG. **5**, as a result of the sub-sampling selection logic **325**, six symbols are selected for processing by the sub-sampled Maximum-Likelihood phase estimation block **326**. In general, the sub-sampled Maximum-Likelihood phase estimation block **326** is configured to perform Maximum-Likelihood operations using the six selected symbols (symbols R**2**', R**3**', R**5**', R**7**', R**9**', and R**11**') to generate a Maximum-Likelihood phase estimates (offset) **332**(**1**)-**332**(**6**) for each group.

At the symbol rotation segment **334**, the Maximum-Likelihood phase estimates **332**(**1**)-**332**(**6**) are then applied to the Viterbi-Viterbi phase error corrected symbols R**1**' though R**12**' in the respective group. More specifically, at the symbol rotation segment **334**, each of the Viterbi-Viterbi phase error corrected symbols R**1**' though R**12**' are provided to an associated processing block **335**(**1**)-**335**(**12**). Each block **335**(**1**)-**335**(**12**) also receives a Maximum-Likelihood phase estimate for the corresponding group. For example, blocks **335**(**1**) and **335**(**2**) receive the Viterbi-Viterbi phase error corrected symbols R**1**' and R**2**', respectively. The blocks **335**(**1**) and **335**(**2**) also receive the Maximum-Likelihood phase estimate **332**(**1**) corresponding to group **330**(**1**) to which symbols R**1**' and R**2**' belong. That is, the Maximum-Likelihood phase estimate **332**(**1**) generated from R**2**' is used for the phase error correction of both symbols R**1**' and R**2**' at the symbol rotation segment **334**. Table 9, below, illustrates the Maximum-Likelihood phase estimate that is used to correct each of the symbols R**1**' through R**12**' at the symbol rotation segment **335**.

TABLE 9

Symbol	Correction Signal
Symbol R1'	332(1)
Symbol R2'	332(1)
Symbol R3'	332(2)
Symbol R4'	332(2)
Symbol R5'	332(3)
Symbol R6'	332(3)
Symbol R7'	332(4)
Symbol R8'	332(4)
Symbol R9'	332(5)
Symbol R10'	332(5)
Symbol R11'	332(6)
Symbol R12'	332(6)

The symbol rotation segment **334** is configured to output a plurality of complete phase error corrected signals, shown in FIG. **5** as symbols R**1**" though R**12**". These symbols R**1**" through R**12**" represent fully phase recovered symbols.

FIG. **6** is a schematic diagram of another two-stage carrier phase estimation with sub-sampled Viterbi-Viterbi and Maximum-Likelihood carrier phase estimation stages in accordance with examples presented herein. More specifically, FIG. **6** illustrates an arrangement where the Viterbi-Viterbi phase estimate is only applied to symbols that will be considered in the Maximum-Likelihood stage behind the Viterbi-Viterbi stage. After the Maximum-Likelihood phase error estimation, the sum of the Viterbi-Viterbi estimate and the Maximum-Likelihood estimate is applied to all corresponding uncorrected symbols (R**1**-R**12**).

FIG. **6** illustrates a Viterbi-Viterbi stage **445** that is substantially similar to the Viterbi-Viterbi stage **245** of FIG. **4**. That is, the Viterbi-Viterbi stage **445** operates as described above to generate the plurality of Viterbi-Viterbi estimated phase corrections from the symbols selected through the sub-sampling techniques, in this case symbols R**1**, R**6**, and R**10**. The generated Viterbi-Viterbi estimated phase corrections generated from R**1**, R**6**, and R**10** are shown in FIG. **6** as Viterbi-Viterbi estimated phase corrections **432**(**1**), **432**(**6**), and **432**(**10**), respectively.

Unlike in the above example of FIG. **4**, the Viterbi-Viterbi stage **445** does not apply the Viterbi-Viterbi estimated phase corrections **432**(**1**), **432**(**6**), and **432**(**10**) to the original symbols R**1**-R**12**. Instead, the Viterbi-Viterbi estimated phase corrections **432**(**1**), **432**(**6**), and **432**(**10**) are provided to a rotation segment **434** coupled to sub-sampling logic **455**. The symbols R**1**-R**12** are grouped in six (6) pairs. The sub-sampling logic **455** operates to select the symbol from each pair that, as detailed above, has highest ratio between the measured signal phase error and additive noise (outmost ring). Only the six symbols selected by the sub-sampling logic **455** receive Viterbi-Viterbi phase correction at rotation segment **434**.

The rotation segment **434** generates six Viterbi-Viterbi phase error corrected symbols, namely R**1**', R**3**', R**5**', R**7**', R**10**', and R**11**' that correspond to the symbols selected by the sub-sampling logic **455**. These Viterbi-Viterbi phase error corrected symbols are provided to Maximum-Likelihood stage **450** that comprises a decision segment **481**, multiplication segment **482**, an adder tree segment **483**, and a vector-to-angle conversion segment **484**. The segments **481**, **482**, **483**, and **484** collectively operate to generate six Maximum-Likelihood estimated phase corrections, shown in FIG. **6** as **470**(**1**), **470**(**3**), **470**(**5**), **470**(**7**), **470**(**10**), and **470**(**11**) that correspond to Viterbi-Viterbi phase error corrected symbols, namely R**1**', R**3**', R**5**', R**7**', R**10**', and R**11**', respectively.

Also shown in FIG. **6** is a correction block **485** that comprises an estimate addition segment **486**, an angle-to-vector conversion segment **488**, and a rotation segment **490**. The estimate addition segment **484** sums the Viterbi-Viterbi estimated phase corrections **432**(**1**), **432**(**6**), and **432**(**10**) and the corresponding Maximum-Likelihood estimated phase corrections **470**(**1**), **470**(**3**), **470**(**5**), **470**(**7**), **470**(**10**), and **470**(**11**) (i.e., generates combined estimated phase corrections). After angle-to-vector conversion segment **488**, the combined estimated phase corrections are applied to all corresponding uncorrected symbols (R**1**-R**12**) at rotation segment **490** to generate fully phase recovered symbols R**1**"-R**12**".

FIG. **7** is a flowchart of a method **600** in accordance with examples presented. Method **600** begins at **605** where a plurality of consecutive symbols associated with an optical signal received at an optical receiver is obtained. For example, the optical signal was transmitted over an optical fiber span by a transmitter and received at the optical receiver. At **610**, carrier phase recovery of the optical signal is performed using one or more carrier phase estimation stages. At **615**, a subset of the plurality of consecutive symbols is selected for use in carrier phase estimation. The subset of symbols selected for use in carrier phase estimation at each of the one or more stages comprises symbols that provide the most phase information about the optical signal that is relevant for phase error estimation in each of the one or more stages.

In certain examples, the one or more carrier phase estimation stages include a Viterbi-Viterbi carrier phase estimation stage that generates Viterbi-Viterbi phase error corrected symbols. In such embodiments, the selection of the subset of the plurality of consecutive symbols for carrier phase estimation may include performing ring partitioning of the symbols to determine within which of a first, second, or third constellation radius ring each of the symbols falls, organizing the plurality of consecutive symbols into a plurality of groups, and selecting, from each of the plurality of groups, a symbol that has the highest ratio between the measured signal phase error and additive noise and is useable in a given phase error estimation stage.

The above description is intended by way of example only.

What is claimed is:

1. A method comprising:

obtaining a plurality of consecutive symbols associated with an optical signal received at an optical receiver;

performing carrier phase recovery of the optical signal using one or more carrier phase estimation stages to generate a phase recovered signal; and

at each of the one or more carrier phase estimation stages, selecting a subset of the plurality of consecutive symbols for use in carrier phase estimation, wherein the subset of symbols selected for use in carrier phase estimation at each of the one or more stages comprises one or more symbols having a highest ratio of measured signal phase error to additive noise.

2. The method of claim **1**, wherein performing carrier phase recovery of the optical signal using one or more carrier phase estimation stages comprises:

performing carrier phase recovery using a Viterbi-Viterbi carrier phase estimation stage to generate Viterbi-Viterbi phase error corrected symbols.

3. The method of claim **2**, wherein selecting a subset of the plurality of symbols for carrier phase estimation comprises:

performing ring partitioning of the symbols to determine within which of a first, second, or third constellation radius ring each of the symbols falls;

organizing the plurality of symbols into a plurality of groups of symbols consecutive in time;

discarding any symbols which fall in the second ring and are not usable in a 4^{th}-power function; and

selecting, from the symbols remaining in each of the plurality of groups, a symbol that has the highest ratio between measured signal phase error and additive noise.

4. The method of claim **2**, wherein performing carrier phase recovery of the optical signal using one or more carrier phase estimation stages comprises:

performing carrier phase recovery using a Maximum-Likelihood carrier phase estimation stage, wherein the Maximum-Likelihood carrier phase estimation stage operates using a subset of the Viterbi-Viterbi phase error corrected symbols.

5. The method of claim **4**, wherein selecting a subset of the plurality of symbols for carrier phase estimation comprises:

organizing the plurality of Viterbi-Viterbi phase error corrected symbols into a plurality of groups of symbols consecutive in time; and

selecting, from each of the plurality of groups of Viterbi-Viterbi phase error corrected symbols, a symbol with the highest ratio between measured signal phase error and additive noise.

6. The method of claim **4**, wherein selecting a subset of the plurality of symbols for carrier phase estimation comprises:

organizing the plurality of Viterbi-Viterbi phase error corrected symbols into a plurality of groups;

discarding any Viterbi-Viterbi phase error corrected symbols for which a precursor of the Viterbi-Viterbi phase error corrected symbols was used in the Viterbi-Viterbi carrier phase estimation stage; and

selecting, from the one or more symbols remaining in each of the plurality of groups of Viterbi-Viterbi phase error corrected symbols, a Viterbi-Viterbi phase error corrected symbol with the highest ratio between the measured signal phase error and additive noise.

7. The method of claim **1**, further comprising:

decoding the phase recovered signal with a forward error correction decoder.

8. An apparatus comprising:

a phase recovery module configured to perform carrier phase estimation using one or more stages; and

sub-sampling logic configured to receive a plurality of consecutive symbols associated with an optical signal and configured to select a subset of the plurality of consecutive symbols for use in carrier phase estimation to obtain a phase recovered signal, wherein the subset of symbols selected for use in carrier phase estimation at each of the one or more stages comprise one or more symbols having a highest ratio of measured signal phase error to additive noise.

9. The apparatus of claim **8**, wherein the phase recovery module comprises a Viterbi-Viterbi carrier phase estimation stage configured to generate Viterbi-Viterbi phase error corrected symbols.

10. The apparatus of claim **9**, wherein the sub-sampling logic is configured to:

perform ring partitioning of the symbols to determine within which of a first, second, or third constellation radius ring each of the symbols falls;

organize the plurality of symbols into a plurality of groups of symbols consecutive in time;

discard any symbols which fall in the second ring and are not usable in a 4^{th}-power function; and

select, from the symbols remaining in each of the plurality of groups, a symbol that has the highest ratio between measured signal phase error and additive noise.

11. The apparatus of claim **9**, wherein the phase recovery module further comprises a Maximum-Likelihood carrier phase estimation stage, wherein the Maximum-Likelihood carrier phase estimation stage operates using a subset of the Viterbi-Viterbi phase error corrected symbols.

12. The apparatus of claim **11**, wherein the sub-sampling logic is configured to:

organize the plurality of Viterbi-Viterbi phase error corrected symbols into a plurality of groups of symbols consecutive in time; and

select, from each of the plurality of groups of Viterbi-Viterbi phase error corrected symbols, a symbol with the highest ratio between measures signal phase error and additive noise.

13. The apparatus of claim **11**, wherein the sub-sampling logic is configured to:

organize the plurality of Viterbi-Viterbi phase error corrected symbols into a plurality of groups;

discard any Viterbi-Viterbi phase error corrected symbols for which a precursor of the Viterbi-Viterbi phase error corrected symbols was used in the Viterbi-Viterbi carrier phase estimation stage; and

select, from the one or more symbols remaining in each of the plurality of groups of Viterbi-Viterbi phase error corrected symbols, a Viterbi-Viterbi phase error corrected symbol with the highest ratio between the measured signal phase error and additive noise.

14. The apparatus of claim **8**, further comprising a forward error correction decoder configured to decode the phase recovered signal.

15. A method comprising:

obtaining a plurality of consecutive symbols associated with an optical signal received at an optical receiver;

grouping the plurality of consecutive symbols into a plurality of groups of symbols consecutive in time; and

from each of the plurality of groups, selecting the symbol having a relative highest ratio between measured signal phase error and additive noise to generate a subset of received symbols; and

performing carrier phase recovery at one or more carrier phase estimation stages using the subset of received symbols to obtain a phase recovered signal.

16. The method of claim **15**, wherein performing carrier phase recovery of the optical signal using one or more carrier phase estimation stages comprises:

performing carrier phase recovery using a Viterbi-Viterbi carrier phase estimation stage to generate Viterbi-Viterbi phase error corrected symbols.

17. The method of claim **16**, wherein selecting the symbol having the relative highest ratio between the measured signal phase error and additive noise to generate a subset of received symbols comprises:

performing ring partitioning of the symbols to determine within which of a first, second, or third constellation radius ring each of the symbols falls;

organizing the plurality of symbols into the plurality of groups of symbols consecutive in time; and

selecting, from each of the plurality of groups, a symbol that that has the highest ratio between the measured signal phase error and additive noise and is useable in a 4^{th}-power function.

18. The method of claim **16**, wherein performing carrier phase recovery of the optical signal using one or more carrier phase estimation stages comprises:

performing carrier phase recovery using a Maximum-Likelihood carrier phase estimation stage, wherein the

Maximum-Likelihood carrier phase estimation stage operates using a subset of the Viterbi-Viterbi phase error corrected symbols.

19. The method of claim **18**, further comprising:

organizing the plurality of Viterbi-Viterbi phase error corrected symbols into a plurality of groups;

discarding any Viterbi-Viterbi phase error corrected symbols for which a precursor of the Viterbi-Viterbi phase error corrected symbols was used in the Viterbi-Viterbi carrier phase estimation stage; and

selecting, from the one or more symbols remaining in each of the plurality of groups of Viterbi-Viterbi phase error corrected symbols, a Viterbi-Viterbi phase error corrected symbol with the highest ratio between the measured signal phase error and additive noise.

20. The method of claim **15**, further comprising:

decoding the phase recovered signal with a forward error correction decoder.

* * * * *